CALCULATION OF THE HYDRODYNAMIC INTERACTION BETWEEN TWO ENCOUNTERING BODIES IN COUPLING MULTI-FREEDOM MOTIONS

(DOI No: 10.3940/rina.ijme.2015.a4.328)

H M WANG, L WANG, L Q TU and **C H ZHAO**, School of Naval Architecture and Ocean Engineering, Zhejiang Ocean University, Key Laboratory of Offshore Engineering Technology of Zhejiang Province, China

SUMMARY

The sway and yaw motion will be induced additionally due to the interaction effects when two encountering bodies sail in close proximity, which may lead to the collision accident. In the present study, two ellipsoids are taken as an example. By coupling the motion equations of the two bodies and the fluid flow equations, the interaction forces and moments are calculated, and the tracks are predicted. The numerical results for the model fixed motion (only free to surge) at constant speed are compared with those published in literature for the validation of the method proposed in this paper, and good agreement is found. On this basis, more complicated multi-degree of freedom motions in surge, sway and yaw directions induced by the interaction effects are simulated. By systematically comparing and analyzing the numerical results obtained at different speeds, lateral distances and body sizes, the influences of speed and lateral distance and body size on the hydrodynamic forces are elucidated.

NOMENCLATURE

a1, a2	Half lengths of big and small ellipsoids respectively (m)
b1, b2	Half breadths of big and small ellipsoids respectively (m)
Sp	Longitudinal distance between the centers of the two ellipsoids (m)
St	Lateral distance between the centers of the two ellipsoids (m)
U1, U2	The speeds of big and small ellipsoids (m/s)
ϕ, θ, ψ	Euler angles representing the rotations about the X-axis, Y-axis and Z-axis respectively (deg)

1. INTRODUCTION

The prediction of the interaction effects between ships was traditionally carried out by experimental method that has a merit of accuracy, but demerit of longer time and higher cost. The earliest ship model test for the overtaking condition in deep water was performed by Newton (1960) [1]. Later, Dand (1981) [2] performed a set of captive-model tests to gain an insight into the hydrodynamic interactions between encountering ships for the cases of encounter, overtaking and a ship passing by a stationary ship. Then, the theoretical calculations based on slender body theory [3], strip theory, boundary element method (BEM) [4] etc. were carried out to simulate the interaction effects between two ships. Typically, the slender body theory proposed by Newman (1969) [5] laid the foundation for the relevant research later. The semi-empirical mathematical models proposed by Varyani et al. (2002, 2004) [6-7] have been widely adopted in the ship handling simulator. Both Li Xue-dong et al (2010) [8] and Chen Xi-de et al. (2013) [9] got the interactional ships' tracks by using this mathematical model. In recent years, with the development of computers, the related numerical methods based on viscous fluid theory are becoming mature. The motion with a significant viscosity influence, e.g. surge and roll etc. can be predicted well. Chen et al. (1999) [10] developed a hybrid RANS method for the computation of ship-fender coupling during berthing operations. Zhang C. X. et al. (2011) [11-12] systematically simulated interaction effects between two KCS models in straight-line motions including the head-on and overtaking condition. In most researches above, the interactional ships were held fixed in sway, heave, roll, pitch, and yaw directions, and only one-degree of freedom motion in surge direction was considered. In fact, when two ships move in close proximity, the asymmetric flow pattern around the ships will induce sway force and yaw moment, which will make two ships off track. So it is necessary to consider the multi-degree of freedom motions to obtain the more practical interaction information. In the present study, by solving the motion equations of the two encountering ellipsoids and the fluid flow equations, the three-degree of freedom motions in the surge, sway and yaw directions are simulated.

2. MATHEMATICAL DESCRIPTIONS

In order to describe the motions of two encountering bodies, the earth fixed coordinate *OXY* and two body-fixed coordinates *o1 x1 y1*, *o2 x2 y2* are defined, as shown in Figure.1 (a). The origin of body-fixed coordinate system is positioned at the centroid of the body. Two ellipsoids with $a_1 / b_1 = a_2 / b_2 = 8.0$ are taken as example. When the interaction effect is gone, the distance that the small ship deviates its parallel course is denoted by Δd, and the final yaw angle is defined by ψ_f, as shown in Figure.1 (b).

The trajectories of two interactional bodies can be calculated though solving the motion equations of bodies (Eqs.(1)-(6)) and the fluid flow equations (Eqs.(7)-(8)), as follows:

$$\dot{\vec{v}}_G = \frac{1}{m}\sum \vec{f}_G \qquad (1)$$

$$\dot{\vec{\omega}}_B = L^{-1}\left(\sum \vec{M}_B - \vec{\omega}_B \times L\vec{\omega}_B\right) \quad (2)$$

where the acceleration $\dot{\vec{v}}_G$ is solved in the earth fixed coordinate system; the angular acceleration $\dot{\vec{\omega}}_B$ is solved in the body fixed coordinate system; m is the mass of the body; $\vec{f}_G$ is the force acting on the body; L is the moment of inertia; M_B is the moment; ω_B is the angular velocity. The subscripts "G", "B" correspond to the variables in the"earth fixed coordinate system" and"body- fixed coordinate system", respectively.

$\vec{M}_B$ is obtained by Eqs. (3) and (4):

$$\vec{M}_B = R\vec{M}_G \quad (3)$$

$$R = \begin{bmatrix} C_\psi C_\varphi & C_\theta S_\psi & -S_\theta \\ S_\phi S_\theta C_\psi - C_\phi S_\psi & S_\phi S_\theta S_\psi + C_\phi C_\psi & S_\phi C_\theta \\ C_\phi S_\theta C_\psi + S_\phi S_\psi & C_\phi S_\theta S_\psi - S_\phi C_\psi & C_\phi C_\theta \end{bmatrix} \quad (4)$$

where R is the transformation matrix, and its elements are the components of the earth fixed unit vectors expressed in the body fixed system; in generic terms, $C_\chi = \cos(\chi)$ and $S_\chi = \sin(\chi)$, the angles ϕ, θ and ψ are positive for the rotations in counterclockwise direction. $\vec{f}_G$ and $\vec{M}_G$ are obtained by integrating the pressure and shear stresses over the body surface.

The $\dot{\vec{v}}_G$ and $\dot{\vec{\omega}}_B$ are used to update the velocity and angular velocity at the next time step, as shown in Eqs. (5) and (6).

$$v^{n+1} = v^n + \left(\dot{\vec{v}}_G\right)^n \Delta t \quad (5)$$

$$\omega^{n+1} = \omega^n + \left(\dot{\vec{\omega}}_B\right)^n \Delta t \quad (6)$$

The governing equations for turbulent flow in present study are the continuity equations for mass conservation and Reynolds-averaged Navier-Stokes equations for momentum transport, as follows:

$$\frac{\partial u_i}{\partial x_i} = 0 \quad (7)$$

$$\rho\frac{\partial u_i}{\partial t} + \rho u_j\frac{\partial u_i}{\partial x_j} = -\frac{\partial p}{\partial x_i} + \frac{\partial}{\partial x_j}\left(\frac{1}{R_n}\frac{\partial u_i}{\partial x_j} - \rho\overline{u_i' u_j'}\right) \quad (8)$$

where u_i are velocity component in x_i directions; p and $-\rho\overline{u_i' u_j'}$ are static pressure and Reynolds stress respectively.

The CFD software FLUENT is used in this paper with FVM (Finite Volume Method) to discretize the governing equations. The influences of turbulence models on the hydrodynamic interaction between two bodies have been investigated systematically in the previous work [11]. So it is omitted here. Closure of the Reynolds stress problem is achieved by using the turbulence model $RNG\ \ k-\varepsilon$; the standard wall function is used to work with the $RNG\ \ k-\varepsilon$ model to deal with the flow in the boundary layer near the wall; the convective terms are discretized using the first order upwind scheme; central difference scheme is utilized for diffusion terms; for the velocity-pressure coupling, *PISO* algorithm is used. The time interval in the computation is Δt =0.002s. Iteration is performed 20 times at each time step.

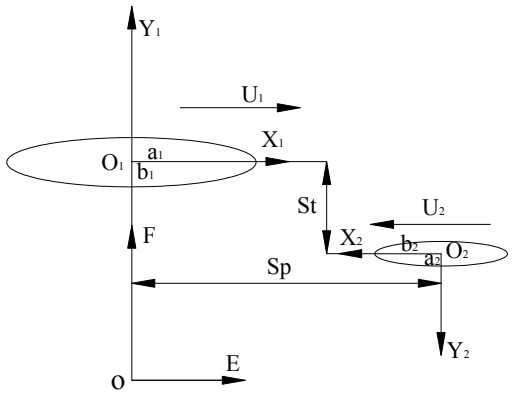

(a) coordinate systems

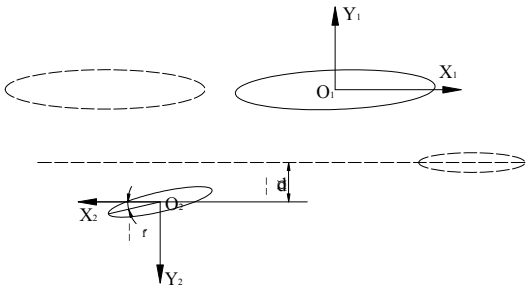

(b) Sketch map for the two encountering ships

Figure 1. Description of the problem

3. NUMERICAL CALCULATIONS

3.1 BOUNDARY CONDITIONS AND GRID GENERATION

An impermeable and no-slip wall boundary condition is set for the rigid body surface; the pressure-outlet condition is set for the inlet and outlet. The hybrid grid technique is employed in the grid generation for the computational domain. Figure 2 shows the global view of the computational grids. Figure 3 shows the layered quadrilateral cells attached the body, which move along the hull and are not regenerated. This can guarantee the quality of the meshes and reduce the time consumption in grid regeneration. The sliding interface technique is used

for data exchange between the moving area and stationary area. Three approaches of mesh updating, namely "Layering", "Smoothing" and "Remeshing"[13], are adopted in the moving area. The "Layering" approach is adopted for the quadrilateral grid area, the "Smoothing" and "Remeshing" approaches are adopted for the triangular grid area. The total number of cells is about 150 000. Convergent numerical results are obtained when the number of cells is about 150 000, and even more.

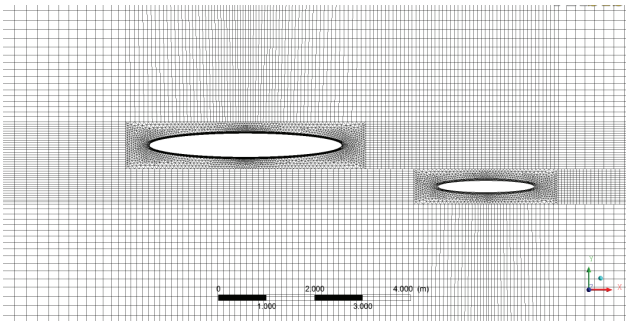

Figure.2 The global view of grids

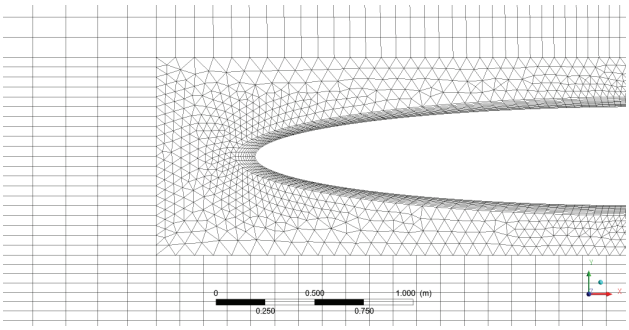

Figure.3 Particular of the grids near the body

3.2 VALIDATION

In order to validate the numerical approach, the cases as same as Collatz's (1963) [14] study are selected, that is, two interactional bodies (*a1*/*a2* = 1) only move along straight courses at constant speed. In order to facilitate the direct comparison with Collatz's data, the sway force and yaw moment are non-dimensionalized by speed, half- breadth of the small body and water density, as the following Eqs.(9) and (10). Positive sway force means attraction and positive yaw moment means the state of "bow-out and stern-in".

Sway force coefficient: $C_y = F_y / \left(\rho b U^2 \right)$ (9)

Yaw moment coefficient: $C_{mz} = M_z / \left(\rho b^2 U^2 \right)$ (10)

In Figure. 4, the sway force and yaw moment coefficients are plotted as function of *Sp/a1* instead of the time history. The domain 0< *Sp/a1*<3 is the stage of approach and -3< *Sp/a1*<0 is departure. The trends are roughly followed, though there are some deviations. The numerically calculated sway force and yaw moment before two heads meet each other show the good agreement with the Collatz's data, but similar agreement does not apply to the departure stage. Because the calculation of Collatz is based on the potential flow theory, the discrepancy of data is most likely due to the effect of the viscous flow effect.

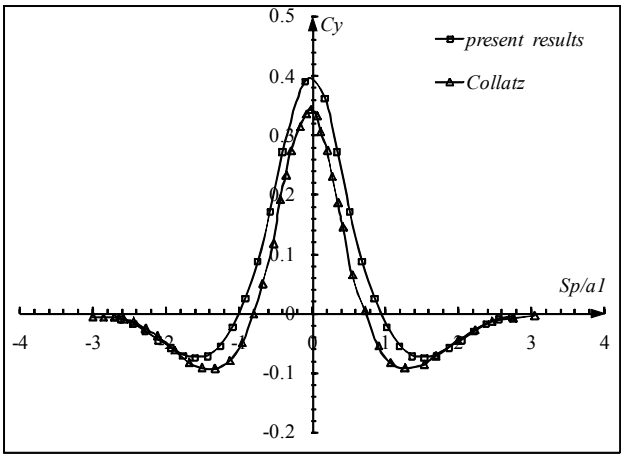

(a) Curves of yaw moment coefficient

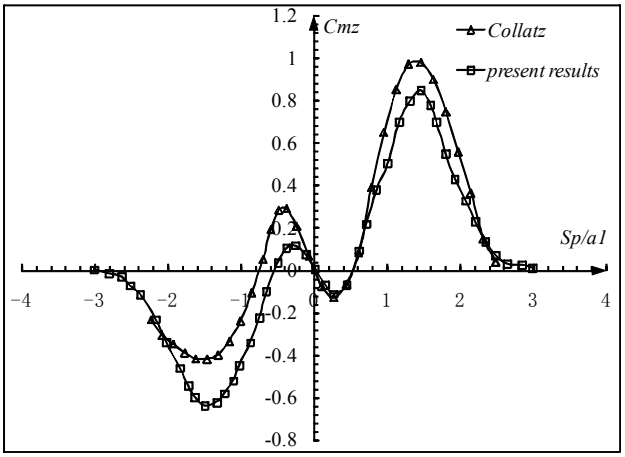

（b）Curves of yaw moment coefficient

Figure.4 Comparison between the present results and Collatz's

3.3 NUMERICAL INVESTIGATION ON MULTI-DOF MOTIONS

The simulation of the multi-DOF motions is more realistic, and the motions in sway and yaw directions may cause the collision accident directly. In the following, the viscous hydrodynamic forces acting on the bodies are calculated by coupling the equations of motions of the bodies and the fluid flow equations. Hereby, the bodies' three-degree of freedom motions in the surge, sway and yaw directions are simulated.

Figure 5 shows the pressure contours at several time instants to illustrate the general flow characteristics around two bodies. It is noted that there is a very strong interaction between two bodies. For the small body, the

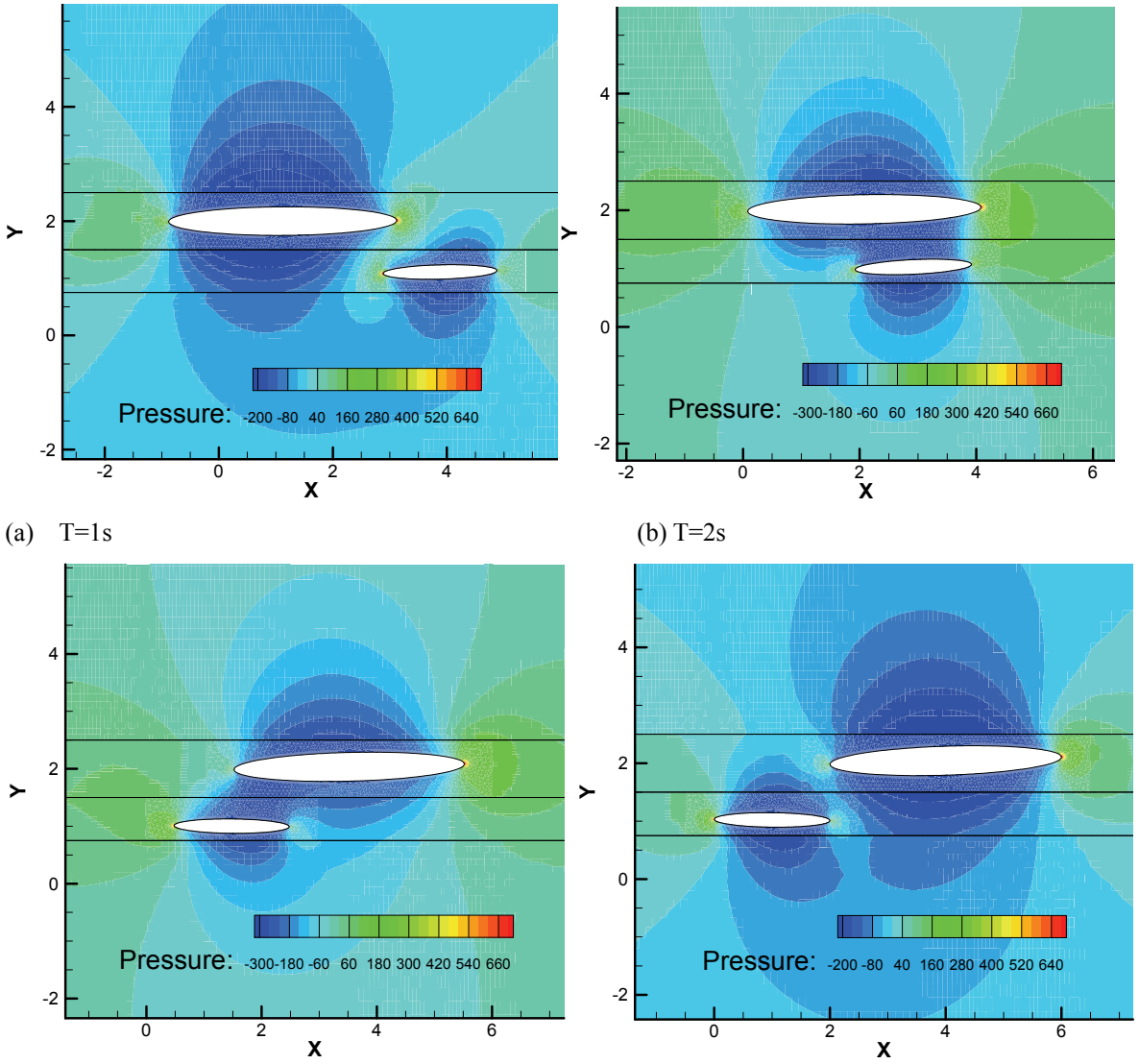

(a) T=1s (b) T=2s

(c) T=3.5s (d) T=4s

Figure.5 Pressure contours around two bodies at several time instants ($a1/a2 = 2$)

pressure on port is smaller than that on starboard as shown in Figure.5 (a), which results in a sharp increasing of the lateral separation distance. An obvious repulsion effect is observed on the small body, as shown in Figure.5 (b). When the bow of the small body is crossing the centroid of the big one, a low-pressure region is developed in the narrow clearance region between two bodies due to the Bernoulli effects, which will lead to the small body's lateral movement towards to big body, as shown in Figure.5 (c). So the small body's movements in sway direction include moving away from the big body firstly and then getting close to the big one. For the big body, its lateral movement is not obvious, and just a small yaw angle appears as shown in Figure.5 (d). During the whole process, the attraction effect is weaker in comparison to the repulsion effect, and the time instant when the small body gets close to the big one is relatively late, nearly passing the big one. So, for the encountering maneuver, due to the initial repulsion, the bodies can pass by each other safely, only slightly deviating from their original straight courses. It is relative safe for both bodies.

The effects of the parameters such as speed, lateral distance and body size on the interaction between two submerged bodies are investigated respectively. Only the sway forces and yaw moments acting on small body are shown in Figures. 6-8. Because the sway force coefficient is obtained by multiplying $1/\rho b_2 U_2^2$ and yaw moment coefficient by $1/\rho b_2^2 U_2^2$ $b2$ and $U2$ should be kept constant to facilitate comparisons. So only the speed of the big body $U1$ is changed when studying the speed effect, and only the big body's half-breath $b1$ is changed when studying the body size effect. In contrast to the case of Collatz's one-degree of freedom motion, the obvious discrepancy can be observed, that is, the sway force coefficient curves are no longer symmetric about the y-axis, which may be attributed to that the circulation about the two bodies is ignored in the Collatz's calculations. Meanwhile, the motions of sway and yaw induced by the interaction effects are also the main contributors for this discrepancy. There is something strikingly different about the curves smoothness compared

with that in the case of Collatz's , which may be attributed to that the smoothness of the flow field detaching from the big body is non-ideal, so the small body sails in the quite complicated flow. Figure.6 shows the sway force and yaw moment coefficients acting on the small body for different relative speeds of two bodies. It is observed that the phase does not change with the body speed, but the peak sway force and yaw moment have multiplied with increasing body speed. For constant *U*2, the maximum sway force $C_{y\max}$ increases linearly with U_1 , that is, $C_{y\max} = \alpha U_1 + \beta$, where the slope α =0.4 and the intercept β = -0.04.The maximum yaw moment shows the similar trends, $C_{mz\max} = \delta U_1 + \varepsilon$, where the slope δ =1 and the intercept ε = -0.5. In Figure.7, the magnitude orders of the peak sway force and yaw moment coefficients are C (St = 8*b2*)< *C*(St = 7*b2*)< *C* (St = 6*b2*), which mean that the smaller lateral distance has a bigger influence on the interaction hydrodynamic forces. For the peak sway force, it increases linearly with the decreasing lateral distance and the similar trend applies to the yaw moment. From Figure 8, it is noted that the effect of body size upon the hydrodynamic forces coefficient seems to be smaller than the other two factors.

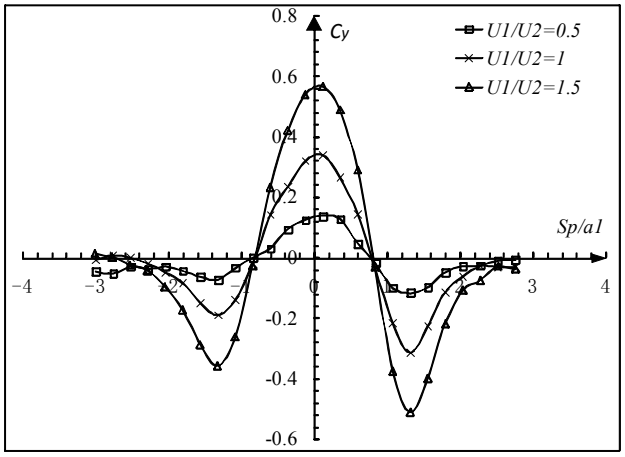

(a) Curves of sway force coefficient

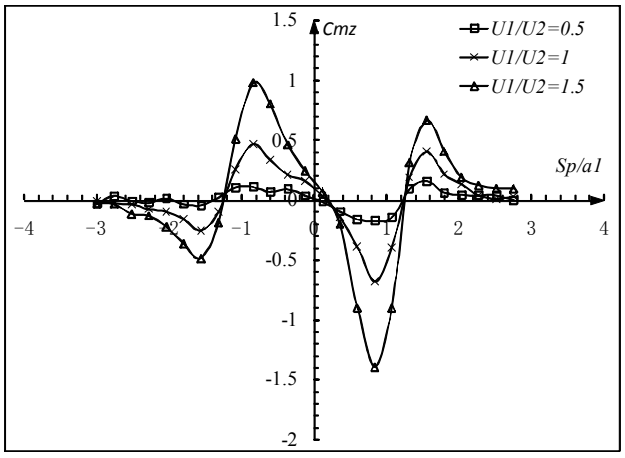

(b) Curves of yaw moment coefficient

Figure 6 Comparison of the hydrodynamic forces on the small body at different speed (*a1*/*a2*= 2, St=6 b_2)

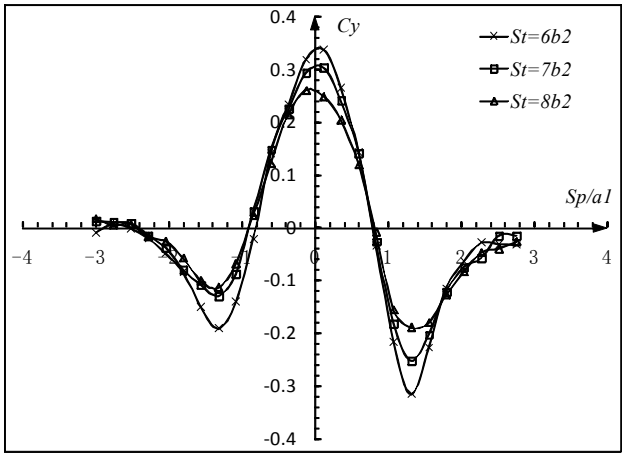

(a) Curves of sway force coefficient

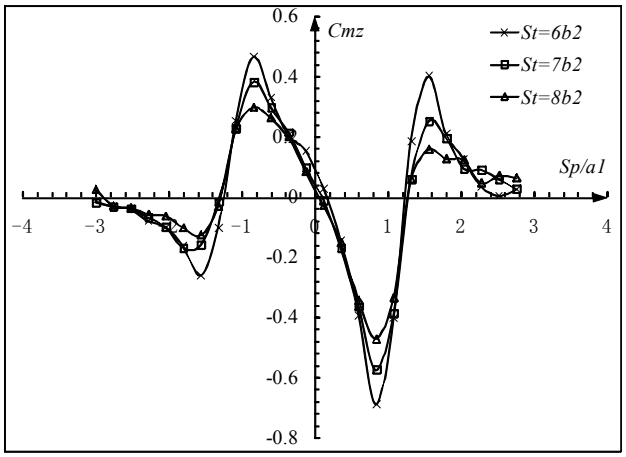

(b) Curves of yaw moment coefficient

Figure 7 Comparison of the hydrodynamic forces on the small body at different lateral distance (*a1*/*a2*= 2, U_1 = -U_2 =1m/s)

The changing of y-coordinates of the two bodies' centroids and yaw angles are shown in Figures 9-10 respectively. In Figure 9, we can see that the variations of the y-coordinates of the two bodies' centroids are quite different. From Figure 9 (a), it can be seen that the y-coordinate decreases until *Sp/a1* = -0.3, and then increases to the position *Sp/a1* = -1.6 where the two bodies have completely passed each other. After that, we can see that the y-coordinate is kept decreasing linearly, and this is because a positive yaw angle ψ_f still exist in this stage. From Figure 9 (b), it can be seen that the y-coordinate increases until *Sp/a1* = -0.3, and then always decreases. Form the Figure 9, it is clearly observed that the two bodies move far away firstly and then close to each other in lateral direction. In Figure 10, it can be seen that ψ_f is nearly constant in the region *Sp/a1* < -2.4 for the small body and *Sp/a1* < -1.8 for the big one, which means the interaction effect on the yaw motion has become negligible, and the two bodies will move at a constant yaw angle ψ_f . From the Figure 10 (a), the yaw angle of the small body during the whole interacting process is always non-negative, which means

the small body is always "bow-out and stern-in". So the interaction effects between two encountering bodies are mainly manifested as the repulsion effect.

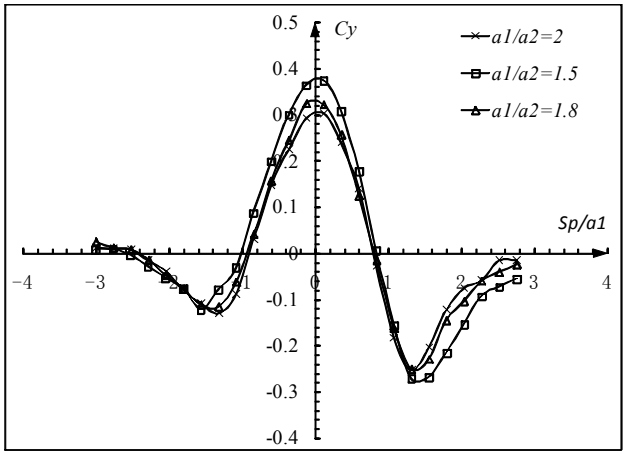

(a) Curves of sway force coefficient

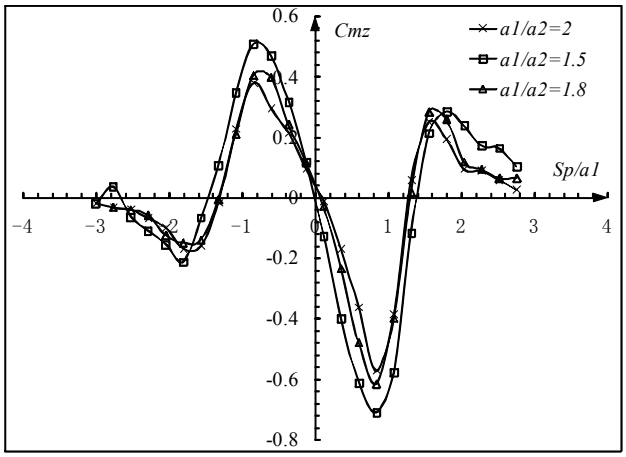

(b) Curves of yaw moment coefficient

Figure 8 Comparison of the sway force and yaw moment on the small body at different body size (St=7 b_2 , U_1 =- U_2 =1m/s)

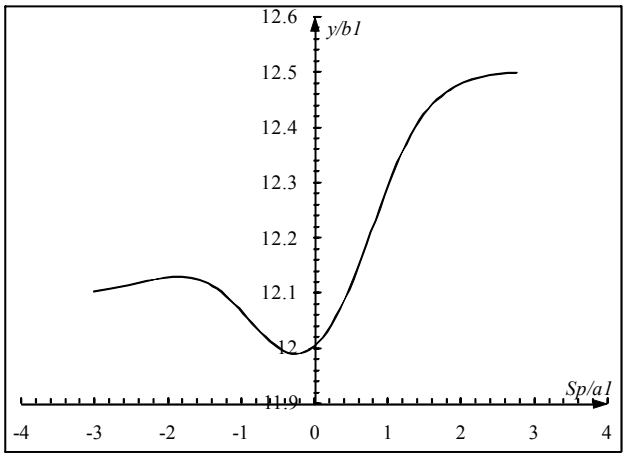

(a) Y-coordinates of the small body's centroid

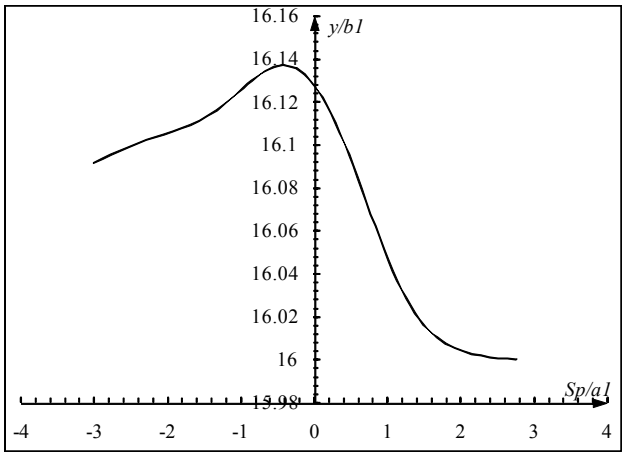

(b) Y-coordinates of the big body's centroid

Figure 9 Variation of the y-coordinates of the two bodies' centroids (St=7 b_2 , U_1 =- U_2 = 1m/s)

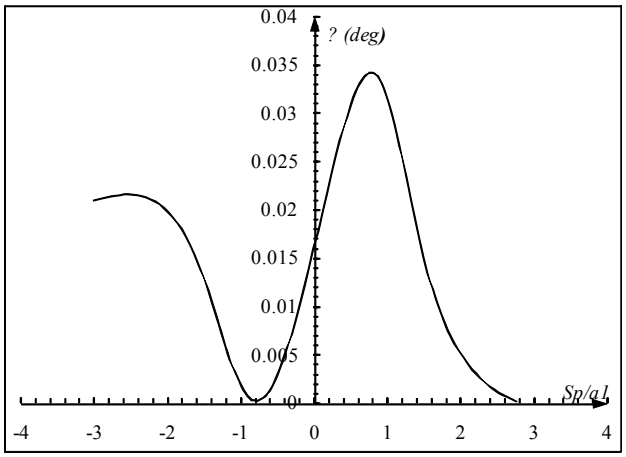

(a) Yaw angle of the small body

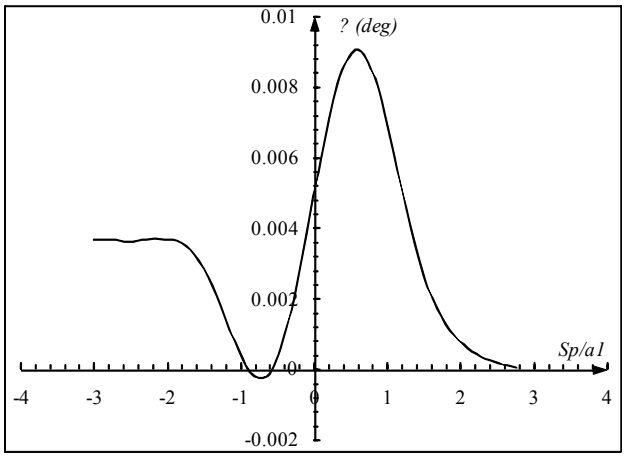

(b) Yaw angle of the big body

Figure 10 Variation of the yaw angles of the two bodies (St=7 b_2 , U_1 = - U_2 = 1m/s)

4. CONCLUSIONS

For safe operation of a submerged body while operating in the proximity of the other, accurate track prediction is very important to the navigator. Currently, the numerical investigations on a more complicated multi-degree of freedom motions induced by the interaction effects are scarce. In this work, by solving the equations of motion of bodies and the viscous fluid flow equations, the flow field around two encountering submerged bodies moving in surge, sway and yaw directions are simulated. Validation of the present numerical approach is performed by comparing with the result published in literature. Several relative speeds, lateral distances and body sizes are considered to examine the sensitivity of these factors to the interaction effects. Some significant results are obtained：a) The interaction effects on small body are remarkable, whereas, for the big body, the effects are negligible; b) The factor of speed can affect the interaction between encountering bodies obviously. The sway force and yaw moment acting on the small body with constant speed nearly increase linearly with the speed of big one; c) The interaction effect of sway force and yaw moment may be aggravated for the smaller lateral distance; d) The body size effect on the interaction is smaller than factors of relative speed and lateral distance.

5. ACKNOWLEDGEMENTS

This work is supported by the National Natural Science Foundation of China (Grant No. 51109186) and Zhejiang Provincial Natural Science Foundations of China (Grant No. LY16E090004, LY14E090003) and the Open Foundation from Key Laboratory of Marine Fishery Equipment and Technology of Zhejiang.

6. REFERENCES

1. NEWTON R.M., Some notes on interactions effects between ships close aboard in deep water, *1. Symp. Naval Manoeuvrability*, Washington, pp.1-24, 1960.
2. DAND, I. W., Some measurements of interaction between ship models passing on parallel courses, *National Maritime Institute, 108*, 1981.
3. DAVIS, A. M. J., and J. F. GEER, The application of uniform-slender-body theory to the motion of two ships in shallow water, *Journal of Fluid Mechanics114, pp. 419-441*, 1982.
4. ZHANG X. D. and LIU Z. Y., Calculation of the interaction forces between ships with one overtaking the other, *Journal of Wuhan Transportation University*, *21,pp. 236-241*, 1997. (in Chinese)
5. NEWMAN, J. N, Lateral motion of a slender body between two parallel walls, *Journal of Fluid Mechanics,39, pp. 97-115*, 1969.
6. VARYANI, K. S., MCGREGOR, R. C., KRISHNANKUTTY, P. and THAVALINGAM, A., New empirical and generic models to predict interaction forces for several ships in encounter and overtaking manoeuvres in a channel, *International shipbuilding progress, 49, pp. 237-262*, 2002 .
7. VARYANI, K. S., THAVALINGAM, A. and KRISHNANKUTTY, P., New generic mathematical model to predict hydrodynamic interaction effects for overtaking maneuvers in simulators, *Journal of marine science and technology, 9, pp. 24-31*, 2004.
8. LI X. D., Modeling and simulation of interaction between ships in restricted water, M.S. Thesis, Dalian Maritime University, 2010. (in Chinese)
9. CHENG X. D., LIU Z. Y., Numerical simulation for the ship-ship overtaking maneuvering, *Proceedings of the 2013 Conference on Ship Hydrodynamics, Xian, pp. 440-448,* 2013. (in Chinese)
10. CHEN, H. C., TUANJIE, L., HUANG, E. T. and DAVIS, D. A., Chimera RANS simulation of ship and fender coupling for berthing operations, *The Proceedings of the 9th. International Offshore and Polar Engineering Conference (ISOPE'99), Brest, France*, 1999.
11. ZHANG C. X., Numerical study on unsteady hydrodynamic interaction between ships, M. E. Thesis, Shanghai Jiaotong University, 2011. (in Chinese)
12. ZHANG C. X. and ZOU Z. J., Numerical study on hydrodynamic interaction between ships meeting in shallow water, *Journal of Ship Mechanics*, *16, pp. 27-35*, 2012.
13. ANSYS Inc., ANASYS FLUENT Users' Guide 14.0, *ANSYS Inc., November 2011.*
14. COLLATZ, G. Potential theoretical study of the hydrodynamic interaction between two ships, *Shipbuilding Engineering Association Yearbook*, *57, pp. 281-329,*1963. (in German)

